

Recent flow and correlation measurements in large and small collision systems with ATLAS

Alexander Kevin Gilbert^{a,*} on behalf of the ATLAS Collaboration

^aAGH University of Kraków,

al. Adama Mickiewicza 30, 30-059, Kraków, Poland

E-mail: axle.nivek@gmail.com

These proceedings present a comprehensive overview of recent ATLAS measurements of collective flow phenomena in a variety of collision systems. Measurements of the mean, variance, and skewness of the distribution of event-by-event per-particle average transverse momentum are reported for Pb+Pb collisions at $\sqrt{s_{NN}} = 5.02$ TeV and Xe+Xe collisions at $\sqrt{s_{NN}} = 5.44$ TeV. These measurements give insight into the nature of the spatial energy fluctuations in the QGP produced in heavy ion collisions. Measurements of the azimuthal anisotropy of high- p_T particles in Pb+Pb collisions, using two and four-particle cumulants are presented. The harmonic flow measurements in high- p_T provide information on the path-length dependence of parton energy loss in the quark-gluon plasma. Two sets of measurements that investigate if the presence of jets affects the flow-like behavior observed in pp collisions are also presented.

42nd International Conference on High Energy Physics (ICHEP2024)
18-24 July 2024
Prague, Czech Republic

*Speaker



1. Introduction

Since harmonic flow was proposed in the 1990s to characterize the collective motion in quark-gluon plasma (QGP) evolution, numerous measurements of the Fourier coefficients of n -harmonic v_n have been conducted. Surprisingly, these coefficients have also been observed to be non-zero in smaller systems such as pp collisions. The ATLAS experiment [1] at the Large Hadron Collider (LHC) has conducted a variety of flow-related measurements in both large and small collision systems, focusing on different aspects of flow and correlations. The recent results in flow and correlation measurements were presented in these proceedings. These measurements together contribute to a more comprehensive picture of flow dynamics across a range of system sizes and energies, helping to disentangle the different sources of azimuthal anisotropies and providing essential benchmarks for theoretical models of QGP formation and evolution.

2. Harmonic flow of high- p_T particles in Pb+Pb at $\sqrt{s_{NN}} = 5.02$ TeV

The ATLAS Collaboration has measured the harmonic flow coefficients, v_n , for charged particles with high transverse momentum p_T in Pb+Pb collisions [2]. These measurements provide information for constraining the path-length dependence of jet quenching. The measurement was performed using Scalar Product method. The results in Figure 1 show that v_n increases with p_T up to approximately 3 GeV, after which it decreases. The increased luminosity in recent data has allowed for better resolution at high p_T , enabling more precise measurements in this region. An important result of this measurement is that at high p_T the values do not settle at zero.

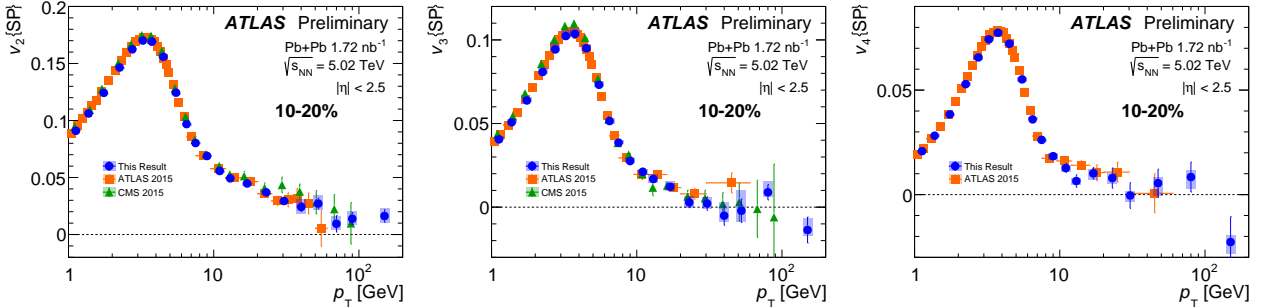


Figure 1: Measurement of v_n as a function of p_T for $n = 2, 3, 4$ from left to right [2].

Additionally, v_n has been studied as a function of centrality. The results in Figure 2 indicate that v_2 increases with centrality, while higher harmonics show a weaker dependence on centrality. Similar trends are observed between v_n measured using particles with low and high p_T .

3. The sensitivity of two-particle correlations in pp collisions to hard scatterings.

Jets and their soft fragments may be correlated with particles in the underlying event. To investigate this, measurements of v_2 from two-particle correlations were carried out in pp collisions at $\sqrt{s} = 13$ TeV, using data corresponding to an integrated luminosity of 15.8 pb^{-1} [3]. These measurements were conducted under two different configurations: first, by excluding charged particles associated with jets from the correlation analysis, and second, by examining correlations

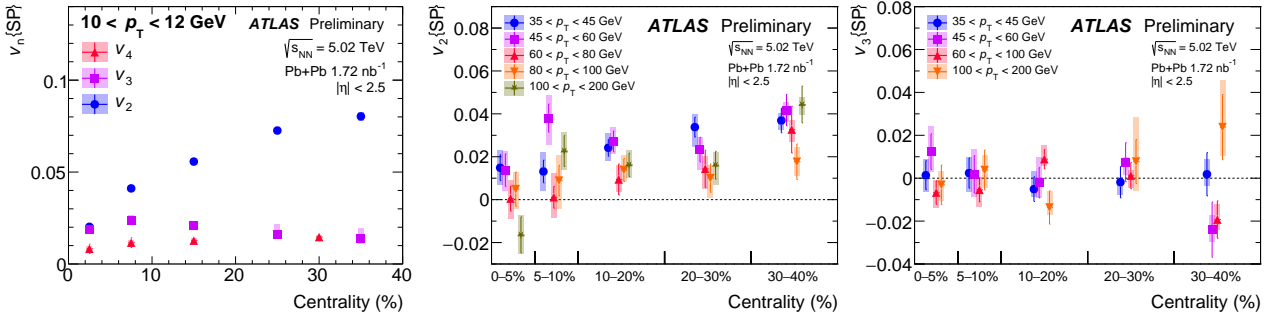


Figure 2: Measurement of v_n as a function of centrality [2].

between particles within jets and charged particles from the underlying event. To minimize the contribution from dijets, the template fitting method is utilized.

Figure 3 shows the measurements of v_2 as a function of event multiplicity and transverse momentum. Excluding particles associated with jets of $p_T > 15$ GeV ($h^{\text{UE}}-h^{\text{UE}}\text{NoJets}$) does not significantly affect the correlations. Additionally, particles associated with jets of p_T exceeding 40 GeV do not exhibit any substantial azimuthal correlations with the underlying event, ruling out hard processes as a source of the ridge effect.

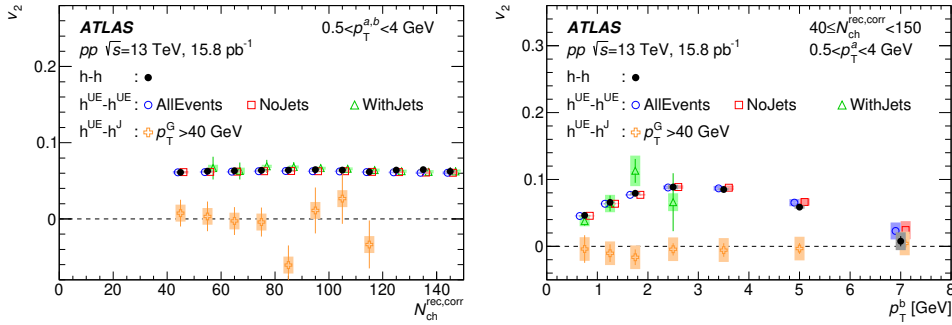


Figure 3: Comparison of v_n as function of charged particle multiplicity (left) and p_T (right) measured in pp collisions at $\sqrt{s} = 13$ TeV with particles associated with jets and those unassociated as indicated by the legend [3].

4. Longitudinal flow decorrelations in pp and Xe+Xe collisions.

In symmetric collision systems, v_n is expected to be the same in the forward and backward η regions. To study this, longitudinal decorrelation parameters F_n are measured [4]. Figure 4 shows the v_n as a function of η before (a_n) and after (c_n) non-flow subtraction (template fitting). The F_n are obtained by fitting

$$v_{n,n}(\eta^a) = A \left(1 + F_n \times (\eta^a) + S_n \times (\eta^a)^2 \right) \quad (1)$$

the coefficients c_n and a_n . The obtained longitudinal decorrelation parameters F_n shown in Figure 5 have non-zero values before and after non-flow subtraction, indicating decorrelation over η . Figure 6 shows the comparison to the AMPT model [5], which reproduces v_n based on spatial eccentricity vectors, avoiding non-flow effects that present in two-particle correlations. The model shows

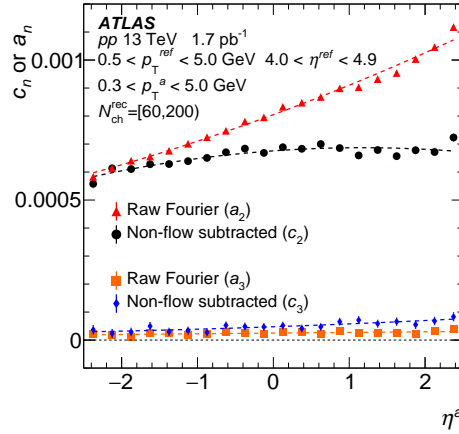


Figure 4: Measurement of v_n as a function η before (a_n) and after (c_n) non-flow subtraction [4].

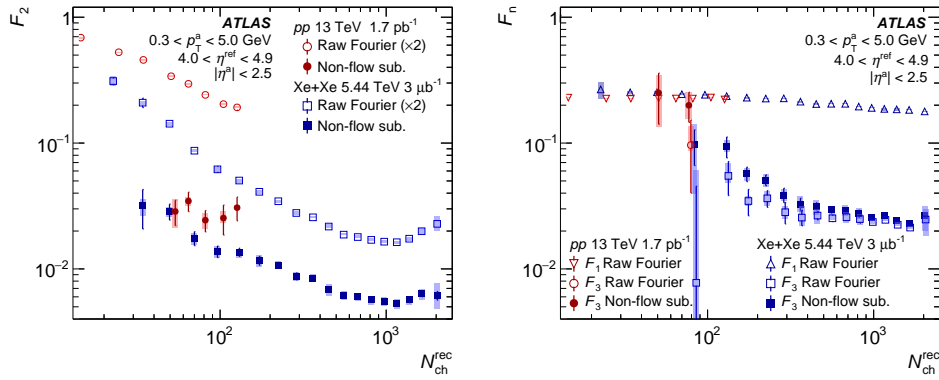


Figure 5: Measurement of F_n for pp and $Xe+Xe$, shown as a function of N_{ch} [4].

qualitative agreement with $Xe+Xe$ data, although it predicts slightly higher values than observed. However, in pp collisions, the model fails to match the experimental data.

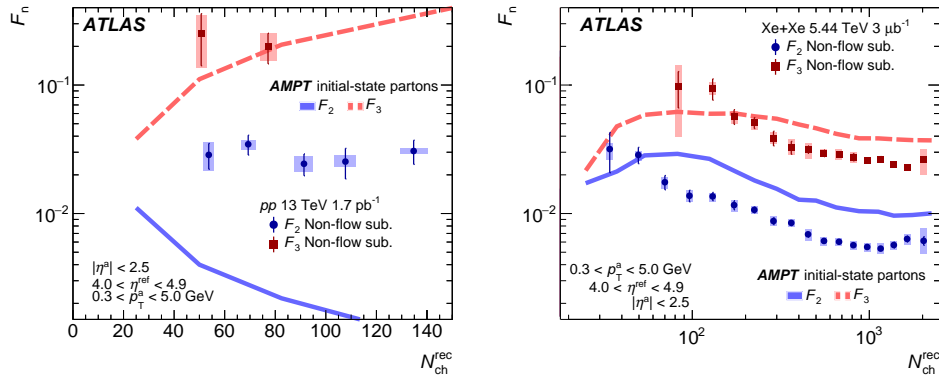


Figure 6: Comparison of the AMPT model predictions (lines) to non-flow subtracted F_n values in in $\sqrt{s} = 13$ TeV pp collisions (left) and $\sqrt{s_{NN}} = 5.44$ TeV $Xe+Xe$ collisions (right) as a function of N_{ch} [4].

5. Momentum fluctuations in Xe+Xe and Pb+Pb collisions

The study of p_T fluctuations in Xe+Xe and Pb+Pb collisions has been performed by ATLAS Collaboration [6]. The mean transverse momentum in a single event, $[p_T] = \frac{\sum_{i_1} w_{i_1} p_{T,i_1}}{\sum_{i_1} w_{i_1}}$, is averaged over an ensemble of events to obtain $\langle [p_T] \rangle$. The variance of n -particle correlation is calculated using

$$c_n = \frac{\sum_{i_1 \neq \dots \neq i_n} w_{i_1} \dots w_{i_n} (p_{T,i_1} - \langle [p_T] \rangle) \dots (p_{T,i_n} - \langle [p_T] \rangle)}{\sum_{i_1 \neq \dots \neq i_n} w_{i_1} \dots w_{i_n}} \quad (2)$$

which are then used to define dimensionless quantities

$$k_2 = \frac{\langle c_2 \rangle}{\langle [p_T] \rangle^2}, \quad k_3 = \frac{\langle c_3 \rangle}{\langle [p_T] \rangle^3}, \quad \gamma = \frac{\langle c_3 \rangle}{\langle c_2 \rangle^{3/2}}, \quad \Gamma = \frac{\langle c_3 \rangle \langle [p_T] \rangle}{\langle c_2 \rangle^2}. \quad (3)$$

These observables are sensitive to radial flow and can be used to measure properties of QGP such as the temperature and speed of sound c_s . The source of $\langle [p_T] \rangle$ fluctuations can be attributed to geometrical factors, such as impact parameter fluctuations, and intrinsic factors that arise from other sources at a fixed impact parameter. In Figure 7, the phenomenological "two-dimensional Gaussian" model [7] reasonably describes the increase in $\langle [p_T] \rangle$ and the corresponding decrease in k_2 , but the larger values of k_3 and Γ observed in the data indicate that additional sources of skewness need to be incorporated into the model.

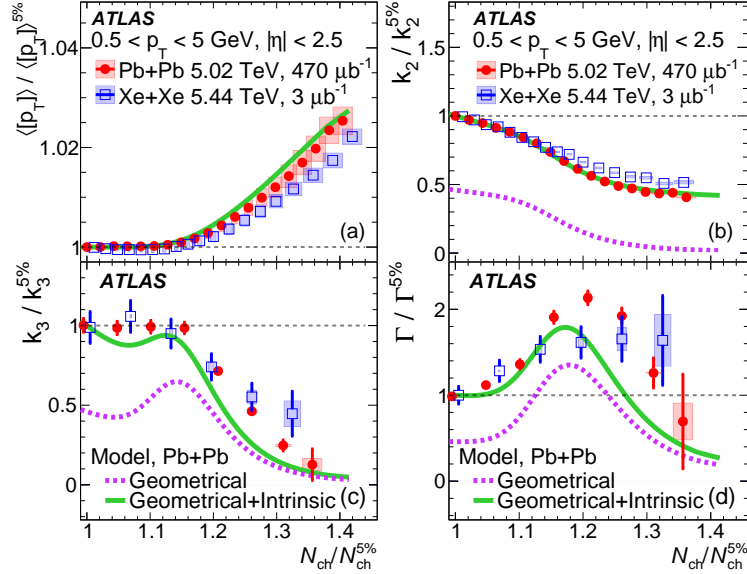


Figure 7: $\langle [p_T] \rangle$, k_2 , k_3 , and Γ normalized by the respective values for 0-5% central events [6].

Figure 8 shows the correlation between $\Delta p_T / \langle [p_T] \rangle$ and $\Delta N_{ch} / N_{ch}$ in the 0-1% most central events, with $\Delta p_T = \langle [p_T] \rangle - \langle [p_T] \rangle_{0-1\%}$ and $\Delta N_{ch} = N_{ch} - \langle N_{ch} \rangle_{0-1\%}$. The positive slope in the relationship between Δp_T and ΔN_{ch} provides information about the speed of sound squared in QGP c_s^2 [8] [9]:

$$c_s^2(T_{\text{eff}}) = \frac{dP}{d\epsilon} = \frac{sdT}{Tds} = \frac{d\langle [p_T] \rangle / \langle [p_T] \rangle}{dN_{ch} / N_{ch}} \approx \frac{\Delta p_T / \langle [p_T] \rangle}{\Delta N_{ch} / \langle N_{ch} \rangle} \quad (4)$$

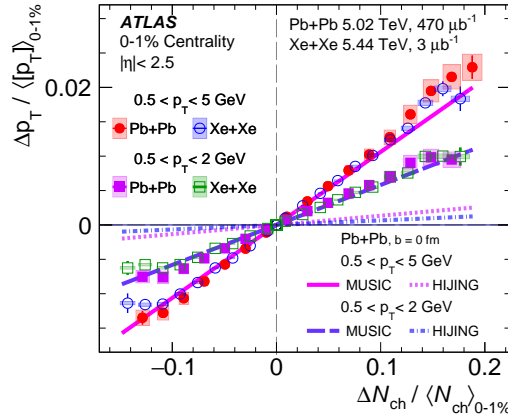


Figure 8: Comparison of correlation between $\Delta p_T / \langle [p_T] \rangle_{0-1\%}$ and $\Delta N_{ch} / \langle N_{ch} \rangle_{0-1\%}$ in data and models [6].

where T is temperature and s is entropy. MUSIC simulations [10] produce a slope similar to that observed in the data, while HIJING [11] underestimates the slope due to its lack of final-state interactions or thermalization mechanisms. The measurement obtains $c_s^2 \approx 0.23$ at $T_{\text{eff}} \approx 222$ MeV.

6. Summary

The increased luminosity allows for greater precision in measuring v_n at high p_T , where the signal predominantly originates from jet fragmentation in Pb-Pb collisions. In pp and Xe-Xe collisions, it is observed that excluding charged particles associated with jets from the correlation analysis does not lead to significant changes in v_n obtained using two-particle correlation. Additionally, there are no observed correlations between jets with $p_T > 40$ GeV and charged particles from the underlying event. The decorrelation in v_n as function of η was measured in Xe-Xe and pp and found to be significant. Furthermore, the study of $[p_T]$ fluctuations in Pb-Pb and Xe-Xe collisions gives the value of $c_s^2 \approx 0.23$ at $T_{\text{eff}} \approx 222$ MeV, as indicated by the agreement between the slopes in Pb-Pb data and the MUSIC model.

7. Acknowledgement

This work was partly supported by the National Science Centre of Poland under grant number UMO-2020/37/B/ST2/01043 and by PL-GRID infrastructure.

References

- [1] ATLAS Collaboration, *JINST* 3 (2008) S08003.
- [2] ATLAS Collaboration, *ATLAS-CONF-2023-007*.
- [3] ATLAS Collaboration, *Phys. Rev. Lett.* 131 (2023) 162301.
- [4] ATLAS Collaboration, Submitted to *Phys. Rev. Lett.*, [arXiv:2308.16745 \[nucl-ex\]](https://arxiv.org/abs/2308.16745).
- [5] Z.-W. Lin, C. M. Ko, B.-A. Li, B. Zhang, and S. Pal *Phys. Rev. C* 72 (2005) 064901
- [6] ATLAS Collaboration, Submitted to *Phys. Rev. Lett.* [arXiv:2407.06413 \[nucl-ex\]](https://arxiv.org/abs/2407.06413).
- [7] R. Samanta, J. P. Picchetti, M. Luzum, and J. Ollitrault, *Phys. Rev. C* 108 (2023) 024908.
- [8] F. G. Gardim, G. Giacalone, and J.-Y. Ollitrault, *Phys. Lett. B* 809 (2020) 135749.
- [9] F. G. Gardim, G. Giacalone, M. Luzum, and J.-Y. Ollitrault, *Nature Phys.* 16 (2020) 615.
- [10] B. Schenke, S. Jeon, and C. Gale, *Phys. Rev. C* 82 (2010) 014903.
- [11] M. Gyulassy and X.-N. Wang, *Comput. Phys. Commun.* 83 (1994) 307.